Lipid Transport Hot Paper

How to cite: *Angew. Chem. Int. Ed.* **2021**, *60*, 19759–19765
International Edition: doi.org/10.1002/anie.202103599
German Edition: doi.org/10.1002/ange.202103599

Synthesis and Cellular Labeling of Multifunctional Phosphatidylinositol Bis- and Trisphosphate Derivatives

*Rainer Müller[+], Ana Kojic[+], Mevlut Citir, and Carsten Schultz**

Abstract: *We synthesized the first multifunctionalized phosphoinositide polyphosphate derivatives featuring a photo-removable protecting group ("cage"), a photo-crosslinkable diazirine group, and a terminal alkyne group useful for click chemistry. We demonstrate that the lipid derivatives readily enter cells. After photo-crosslinking, cell fixation and fluorescent tagging via click chemistry, we determined the intracellular location of the lipid derivatives before and after uncaging of the lipids. We find that there is rapid trafficking of PI(3,4)P_2 and PI(3,4,5)P_3 derivatives to the plasma membrane, opening the intriguing possibility that there is active transport of these lipids involved. We employed the photo-crosslinking and click chemistry functions to analyze the proteome of PI(3,4,5)P_3-binding proteins. From the latter, we validated by RNAi that the putative lipid binding proteins ATP11A and MPP6 are involved in the transport of PI(3,4,5)P_3 to the plasma membrane.*

Introduction

Phosphoinositides are important signaling lipids that contribute to the regulation of many cellular processes including survival, migration, secretion, and growth.[1] The quite abundant phosphatidylinositol 4,5-bisphosphate [PI(4,5)P_2] (ca. 0.1 % of all lipids) was the first phosphoinositide to be recognized as a signaling lipid.[2] The concomitant discovery of phosphatidylinositol 3-kinases (PI3Ks) and phosphatidylinositol 3,4,5-trisphosphate [PI(3,4,5)P_3] in the late 1980ies opened a new field in lipid signaling.[3] Phosphatidylinositol 3,4-bisphosphate [PI(3,4)P_2] was discovered to be a metabolite of PI(3,4,5)P_3 that, however, is now known to trigger its own set of responses.[4] Because it attracts pleckstrin homology (PH) domain-bearing lipid binding proteins to the plasma membrane similar to PI(3,4,5)P_3, the signaling pattern is difficult to distinguish. For instance, both lipids are a sufficient signal for internalization of growth factor receptors, although PI(3,4)P_2 was much less potent than PI(3,4,5)P_3.[5] However, unlike PI(3,4,5)P_3, PI(3,4)P_2 was shown to be involved in the regulation of endosomal trafficking.[4,6]

3-O-phosphorylated phosphoinositide concentrations are only about 0.1 % of that of PI(4,5)P_2 at resting level and are recognized by specific protein domains. Due to the low abundance, it is difficult to determine concentrations of 3-O-phosphorylated PIPs such as PI(3,4,5)P_3, PI(3,4)P_2, and PI(3)P. Typically, fluorescent domain fusion proteins are used to estimate the phosphoinositide levels in intact cells.[7] In cell batches, mass spectrometry is now sensitive enough to detect low levels of these highly charged lipids. However, these techniques come with caveats. For instance, pleckstrin homology (PH) domains do not distinguish well between PI(3,4,5)P_3 and PI(3,4)P_2[8] and mass spectrometry can distinguish between the isomers PI(4,5)P_2 and PI(3,4)P_2 only with difficulties.[9] Even more challenging is the discovery of specific binding proteins of phosphoinositides. We therefore looked for tools that will 1) help to locate the phosphoinositide of interest with high specificity in cells and 2) will at the same time permit finding binding proteins.

We decided to expand our panel of multi-functionalized lipid derivatives to the highly phosphorylated phosphoinositides. In the past, we and others equipped lipids such as cholesterol, sphingosine and diacylglycerol (DAG) with a photo-crosslinking diazirines as well as a terminal alkyne group for click chemistry.[10] Very recently, we equipped phosphatidylinositol with all of the named functional groups.[11] In a typical experiment, cells were incubated with the lipid and illuminated with 350 nm light for crosslinking.[12] Next, cells were fixed and subsequently a fluorophore was attached via click chemistry.[10a,e] Due to the protein-crosslinking, the lipid derivative stayed in place providing a precise location map at the time of crosslinking by fluorescence imaging. Alternatively, we attached biotin to the lipid and lipid-protein conjugates were isolated with streptavidine beads, washed and subjected to proteomic analysis.[10b]

As many lipids experience rapid metabolism inside cells, we equipped each lipid derivative with a photo-activatable protecting group, namely a 7-diethylamino-4-methylene cou-

[*] Dr. R. Müller,[+] Dr. A. Kojic,[+] Dr. M. Citir, Prof. Dr. C. Schultz
European Molecular Biology Laboratory (EMBL), Cell Biology & Biophysics Unit
Meyerhofstr. 1, 69117 Heidelberg (Germany)
Dr. A. Kojic,[+] Dr. M. Citir
Faculty of Biosciences, Collaboration for Joint Ph.D. Degree between EMBL and Heidelberg University
69117 Heidelberg (Germany)
Dr. A. Kojic,[+] Prof. Dr. C. Schultz
Oregon Health & Science University, Department of Chemical Physiology and Biochemistry
3181 SW Sam Jackson Park Rd, Portland, OR 97239-3098 (USA)
E-mail: schulcar@ohsu.edu
[+] These authors contributed equally to this work.
Supporting information and the ORCID identification number(s) for the author(s) of this article can be found under: https://doi.org/10.1002/anie.202103599.

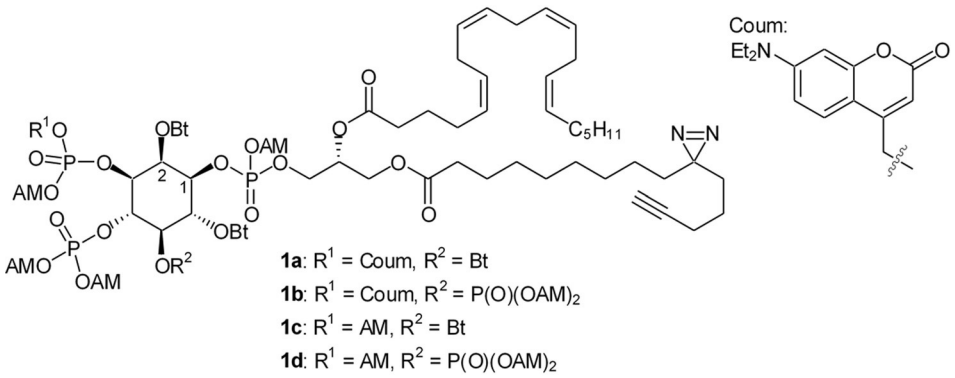

Figure 1. Structures of multifunctionalized PI(3,4)P_2 (**1a**, **1c**) and PI(3,4,5)P_3 (**1b**, **1d**) derivatives featuring both a diazirine and an alkyne group on the *sn*1 fatty acid as well as a photo-activatable coumarin group (cage) on the 3-O-phosphate (**1a**, **1b**). AM = acetoxymethyl, Bt = butyrate.

marin, which is readily removable with 405 nm light.[13] This functional modification gives us excellent access to rapidly elevating the concentration of the lipid species of interest as was shown for many other lipids while preventing premature metabolism.[14] In the past, our group prepared numerous caged phosphoinositides.[11,14b,15] In this work, we will combine photoactivation with photo-crosslinking and fluorescent tagging. We previously demonstrated that 405 nm light is unable to induce significant crosslinking of a diazirine, making the two photochemical reactions subsequently applicable.[12] Unlike many other lipids, most phosphoinositides carry numerous phosphates with negative charges which make cell entry impossible. We therefore needed to apply bioactivatable protecting groups such as acetoxymethyl esters that are easily and rapidly removable by endogenous esterases inside cells.[16]

In this work, we present the synthesis of truly multifunctional phosphoinositide derivatives with all the above named features combined in one molecular tool (Figure 1). We show that the derivatives are biologically fully functional, for instance by inducing growth factor receptor endocytosis after photoactivation. We demonstrate not only spatial lipid distribution but also perform pulse-chase experiments by using rapid photoactivation.

Results and Discussion

The synthetic strategy for preparing multifunctionalized phosphoinositide derivatives was exemplified in our recent synthesis of trifunctional phosphatidylinositol.[11] In brief, the photo-crosslinking diazirine and the alkyne group are both located in one of the two fatty acids. In order to be close to a natural fatty acid composition, we placed the functional groups on the saturated *sn1* fatty acid and kept the arachidonic acid in the *sn2* position unaltered. The resulting diacylglycerol (DAG) derivative is coupled to an already caged head group. In the case of PI(3,4,5)P_3, this head group featured a 7-diethylamino-4-methylene coumarin photoactivatable group at the functionally crucial 3-*O*-phosphate of the inositol moiety and was previously used for caging phosphoinositides.[11,15] In this work, we used a slightly improved synthetic procedure for the synthesis of the phosphoinositide head group that included the use of fluorenylmethyl (Fm) groups for protecting the phosphates. Detailed synthetic procedures (Scheme S1) are described in the supplement. Head group and DAG moiety were coupled to form the fully protected lipid derivative by using an Fm-bearing phosphoramidite that was first reacted with the DAG and subsequently with the inositol head group. After oxidation to the phosphate triester, all phosphate protecting groups were gently removed and alkylation with acetoxymethyl bromide afforded the membrane-permeant bioactivatable lipid derivative.

For the synthesis of a trifunctional PI(3,4)P_2 derivative, the head group synthesis (Scheme 1) required a different synthetic path than for previously non-caged PI(3,4)P_2 derivatives,[17] in order to regioselectively introducing the photoactivatable coumarin moiety to the 3-phosphate. We started from the commercially available enantiopure 2,3:5,6-di*iso*propylidene-*myo*-inositol **2**. Protection of the sterically less restricted 1-hydroxyl group by the bulky TBDPS group afforded alcohol **3**. The single alcohol was protected to give the *p*-methoxybenzyl ether **4**. The more labile ketal was removed and the two hydroxyl groups of **5** were esterified with butyric anhydride to give dibutyrate **6**. The PMB group was removed and alcohol **7** was phosphorylated using the known di(fluorenylmethyl)phosphoramidite **8** to afford **9**. Removal of the ketal liberated the 2- and 3-hydroxyl groups (compound **10**). The thermodynamically less stable 2-OH group was regioselectively esterified using a butyrate orthoester and selective acid-catalyzed ring-opening using Dowex in its protonated form. The resulting tributyrate **11** was subsequently phosphitylated with the known coumarin-bearing P^{III} reagent **12** and oxidized to the bisphosphate triester **13**. Finally, the TBDPS group was removed using 3HF*NEt_3. This latter reaction was tricky because the coumarin group on the phosphate is an excellent leaving group. Accordingly, we isolated the head group **14** in only 23% yield (total yield from **2**: 8.3%). The synthesis of the corresponding head group for PI(3,4,5)P_3 derivatives was performed similar to our previously described path.[15a] Improvements and additional details we describe in the supplement (Scheme S1).

Diacylglycerol **16** was reacted to the Fm-protected phosphoramidite **17**, as described previously (Scheme 2B).[11] Subsequently the inositol headgroups **14** and **15** were coupled to the lipid reagent **17**, to give the fully protected PI(3,4)P_2 (**18a**) and PI(3,4,5)P_3 (**18b**) derivatives, respectively. Deprotection of the Fmoc and Fm groups in one step afforded the desired caged lipids **19a** and **19b.** Both were alkylated with acetoxymethyl bromide to give the bioactivatable caged lipid derivatives **1a** and **1b**, respectively. In the case of PI(3,4)P_2 deprotection, a fraction of the molecules lost the coumarin

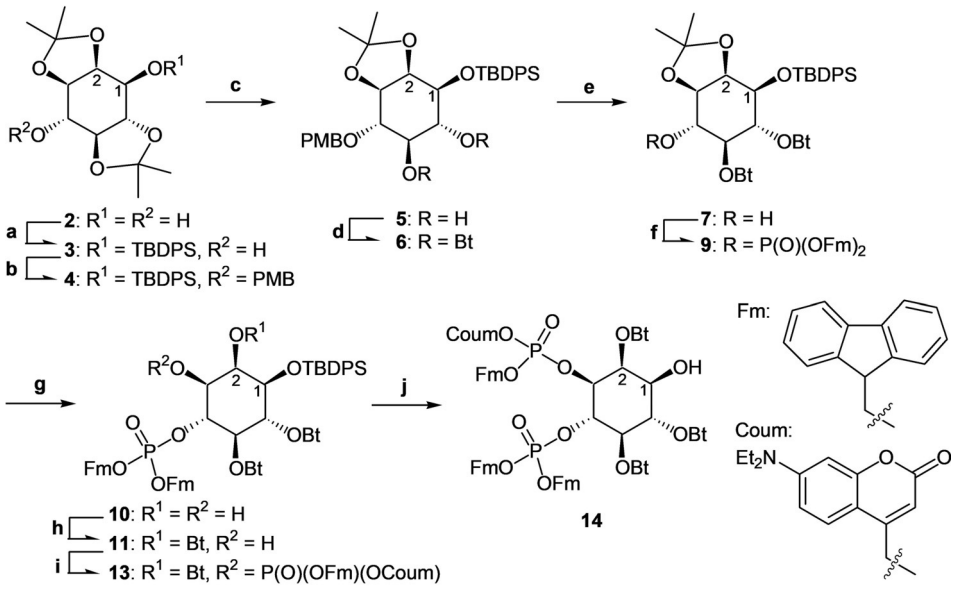

Scheme 1. Synthesis of the caged PI(3,4)P_2 head group. Reagents and conditions: a) TBDPS-Cl, imidazole, pyridine, −10 °C (25); b) PMB-O(C=NH)CCl_3, Et*N*iPr_2, *N*,*N*-dimethylformamide, 22 °C, 18 h; c) CH_2Cl_2:HCOOH 4:1, 22 °C, 2 h, 70% (plus 30% recovery of starting material); d) Bt_2O, di*iso*propylcarbodiimide, 4-dimethylaminopyridine, CH_2Cl_2, 22 °C, 3 h, 87%; e) 2,3-dichloro-5,6-dicyano-1,4-benzoquinone; f) 1 *i*Pr_2NP(OFm)$_2$ (**8**), 1*H*-tetrazole, CH_2Cl_2, 22 °C, 8 h, 2 AcO_2H/AcOH, −78–22 °C, 1 h, 90% yield over two steps; g) CH_2Cl_2:HCOOH 5:95, 22 °C, 2 h, 100%; h) 1. n-$C_3H_7C(OMe)_3$, poly(4-vinylpyridinium) trifluoroacetate, CH_2Cl_2, 22 °C, 18 h; 2. DOWEX H^+, MeCN, H_2O, 100% yield over two steps; i) 1. *i*Pr_2NP(OFm)(OCoum) (**12**), 1*H*-tetrazole, CH_2Cl_2, 22 °C, 8 h, 2. AcO_2H/AcOH, −78–22 °C, 1 h, 90% yield over two steps; j) 3 HF·NEt_3, MeCN, 18 h, 55%. Bt = C_3H_7CO-; PMB = p$MeOC_6H_4CH_2$-; TBDPS = -$SiPh_2t$Bu.

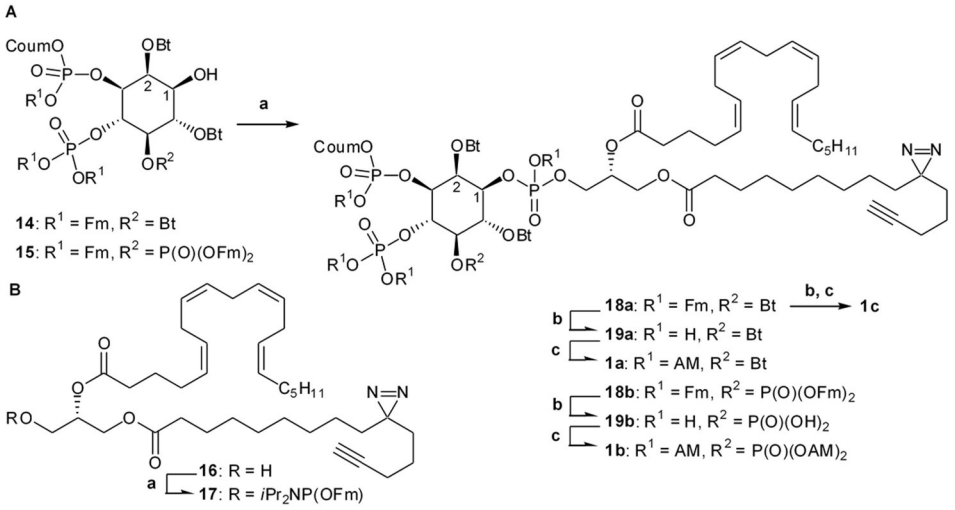

Scheme 2. Coupling of building blocks 14/15 and 17 by P^{III} chemistry, followed by deprotection and alkylation of the phosphates with acetoxymethyl bromide. Reagents and conditions: A for **1a** and **1c**: a) 14, 17, 1*H*-tetrazole, CH_2Cl_2, 23 °C, 5 h; 2. AcO_2H/AcOH, −78–23 °C, 1 h, 86% over two steps; b) Me_2NEt, MeCN, 23 °C, 0.5 h; c) $AcOCH_2Br$, iPr_2NEt, MeCN, 23 °C, 21 h, 50% for **1a** and 24% for **1c** over two steps. A for **1b**: a) 15, 17, 1*H*-tetrazole, CH_2Cl_2, 23 °C, 22 h; 2. AcO_2H/AcOH, −78–22 °C, 1 h, 50% over two steps; b) Me_2NEt, MeCN, 21 °C, 10 min; c) $AcOCH_2Br$, iPr_2NEt, MeCN, 22 °C, 22 h, 23% over two steps. B a) (iPr_2N)$_2$POFm, 1*H*-tetrazole, CH_2Cl_2, NEt_3, 22 °C, 2 h, 89%. Bt = C_3H_7CO-; AM = -CH_2OAc.

group. The following alkylation with acetoxymethyl bromide produced the PI(3,4)P_2 derivative **1c** without caging group but membrane-permeant and with the diazirine and the alkyne in the *sn*1 fatty acid. The synthesis of the respective uncaged PI(3,4,5)P_3 derivative **1d** is described in the supplementary material (Scheme S1).

The caged phosphoinositide derivatives were tested for cell entry and removal of the photoactivatable protecting group ("uncaging"). The latter was achieved by illuminating a 10 mM sample (1 nmol in total) of **1a** or **1b** (Figure 2), for 2 min in a test tube by a 1000 W lamp (Newport) equipped with a 400 nm longpass filter.

Cell entry and fluorescence levels of the caged compounds **1a** and **1b** were quite similar. The compounds entered cells within a couple of minutes. Maximal fluorescence levels were already reached after about 1 min and stayed steady for at least 30 min (Figure 3). The optimal extracellular concentration for observing cell entry of **1a** was at 2 μM, the one for the PI(3,4,5)P_3 derivative **1b** was 5 μM. Lower concentrations led to slower entry while higher ones did not improve loading. Illumination with 375 nm laser light, as is commonly used for the uncaging reaction, lead to a strong but transient increase of the coumarin fluorescence, due to the known phenomenon that the released dye is brighter than its phosphate ester.[11] As was observed before for caged PI and is shown in Figure 3, the caged phosphoinositides accumulated predominantly in the ER and Golgi membrane network. We attribute this localization to an unexplained mechanism that draws lipids bearing aromatic groups into these endomembranes.[11,18] For cell biology experiments, uncaging will provide the 3-phosphorylated phosphoinositides initially at endomembranes. However, the lipids transfer rapidly to the plasma membrane where most of the known biological binding partners and

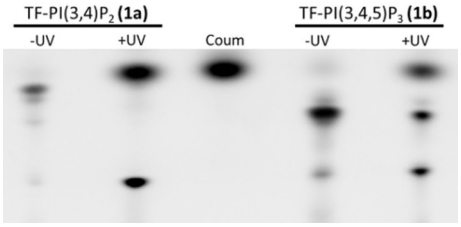

Figure 2. TLC of the non-illuminated and illuminated caged PI derivatives **1a** and **1b** on HPTLC silica 60, eluent chloroform:methanol:water:acetic acid (65:25:4:1) for 6 cm, then cyclohexane:ethyl acetate (1:1) for 9 cm. Prior to TLC lipids were labeled with fluorogenic 3-azido-7-diethylamino coumarin. Middle: 7-diethylamino 4-hydroxymethyl coumarin, the photolyzed "cage group". The lower spots are likely the labeled phosphoinositides after uncaging.

metabolic enzymes such as the phosphatases PTEN and SHIP have been identified.

Our group had previously shown that light-induced release of $PI(3,4,5)P_3$ from membrane-permeant caged $PI(3,4,5)P_3$ derivatives induced clathrin-coated pit-mediated endocytosis of receptor tyrosine kinases such as the epidermal growth factor receptor (EGFR).[5,15a] We therefore incubated HeLa cells with the fluorescent EGFR-GFP fusion, incubated with the trifunctional $PI(3,4,5)P_3$ derivative **1b** and illuminated a subfraction of cells in the field of view with 375 nm blue light to uncage the $PI(3,4,5)P_3$ derivative. Within 30 min, all illuminated cells showed the formation of dotted structures, likely endosomes, while in non-illuminated cells, the fluorescence remained at the plasma membrane (Figure 4). This control experiment demonstrated that the addition of the diazirine and the alkyne did not significantly alter the functionality of the caged $PI(3,4,5)P_3$.

Due to the localization to endomembranes, it is important to show that the lipids are rapidly redistributed after uncaging. While redistribution is suspected because the derivatives are losing their only aromatic moiety, transport proteins are only known for phosphatidylinositol (PI) and PI(4)P but not for higher phosphorylated phosphoinositides.[19]

We therefore made use of the photo-crosslinking properties of the new tools and followed redistribution after uncaging. We first demonstrated that cross-linking led to a much higher retention of the phosphoinositide derivatives

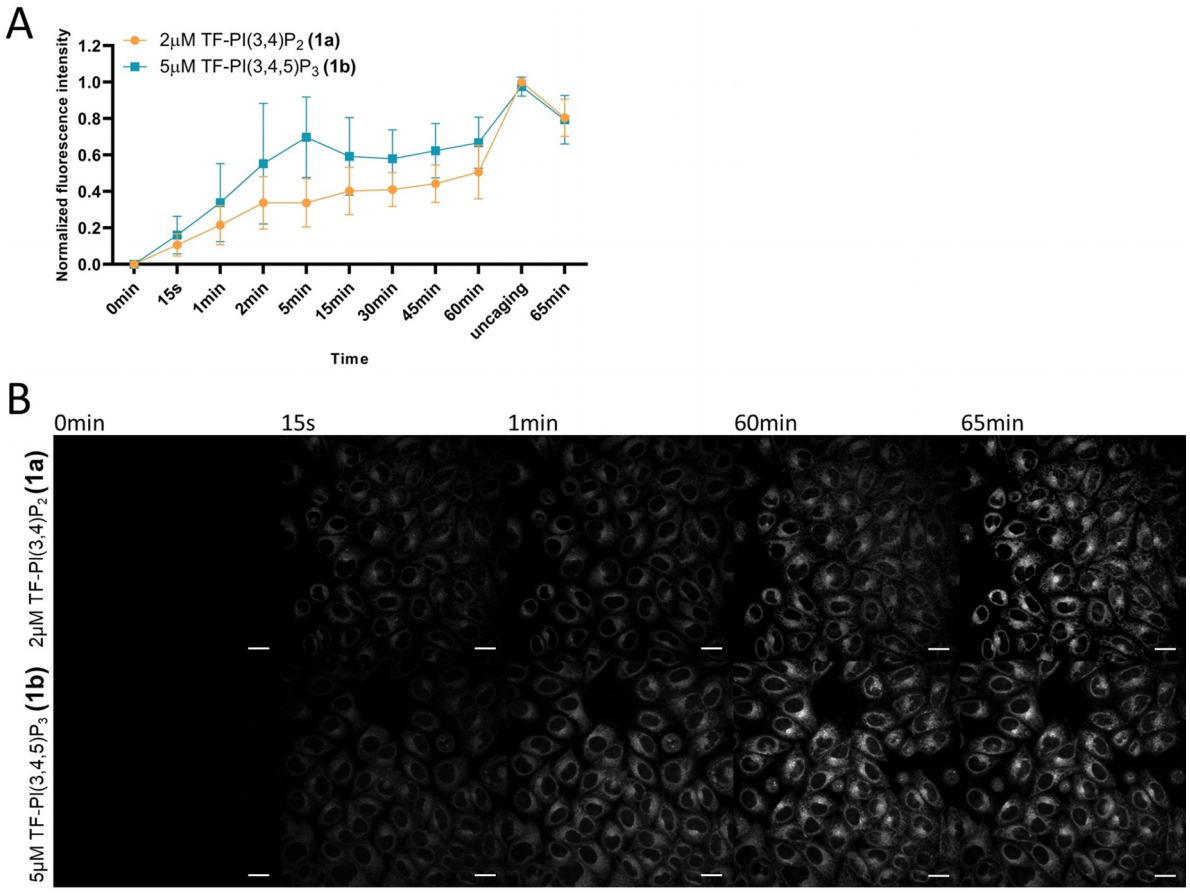

Figure 3. Loading of trifunctional $PI(3,4)P_2$ (2 μM) and $PI(3,4,5)P_3$ (5 μM) derivatives into HeLa cells at 37 °C, respectively (concentrations of 1, 2, 5 and 10 μM were tested, with lower concentrations showing slower compound loading and no further improvement of cell entry with higher concentrations). Illumination of cells with 405 nm laser light after 61 min led to a rapid increase of emission intensity due to the higher quantum yield of the released 7-diethylamino-4-hydroxymethyl-coumarin. Mean values of three replicates were normalized to the maximally observed fluorescence intensity. Error bars are standard deviation. B: selected images following the loading procedure as well as the release of the caging coumarin. Scale bar = 10 μm.

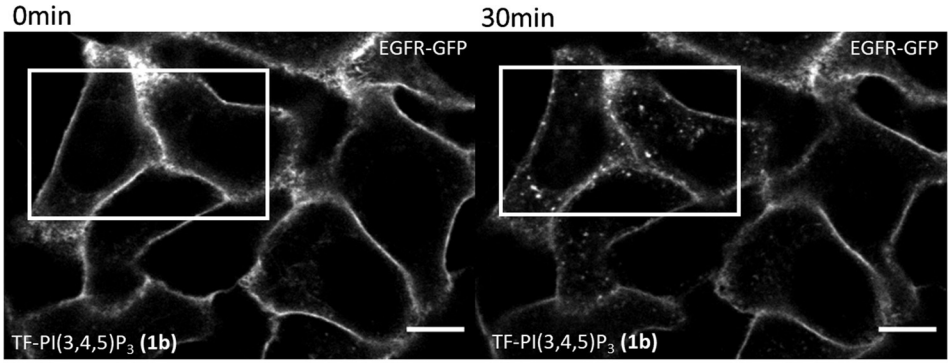

Figure 4. PI(3,4,5)P_3 derivative activity after uncaging. The trifunctional PI(3,4,5)P_3 derivative **1b** fully induced EGFR-GFP internalization in HeLa cells after removal of the photoactivatable protecting group by a 6 s 375 nm light flash shortly after the image on the left was taken. Only illuminated cells (white box) showed EGFR-GFP internalization. These images are representative of three independent experiments. Scale bar = 10 μm.

in HeLa cells compared to when crosslinking was omitted. In this case, most of the lipid was removed in the fixation process (Figure 5A). To look at lipid transport, we uncaged the lipid derivatives prior to photo-crosslinking. We observed a quite rapid appearance of the fluorescence at the plasma membrane (Figure 5B, see the arrows, Figure S1). As this effect was observed after only 30 s, we speculated that active transport might contribute to the change in location. We further showed that crosslinking was specific and can be outcompeted by incubating the cells with a higher dose of a membrane-permeant caged PI(3,4)P_2 or PI(3,4,5)P_3 derivative, respectively, that lack the cross-linking diazirine (Figure S2). We therefore employed the possibility of attaching the cross-linked lipid-protein conjugates to azide beads for subsequent proteomic analysis.

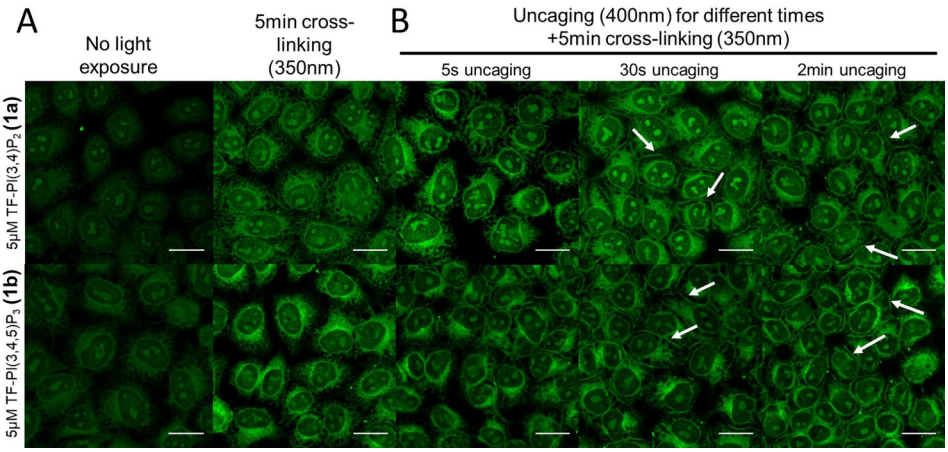

Figure 5. PI(3,4)P_2 and PI(3,4,5)P_3 location. HeLa cells were incubated with 5 μM **1a** or **1b**, respectively, for 5 min and uncaged with > 400 nm light for various time period. Subsequently, cells were photo-crosslinked with 350 nm UV light for 5 min and then fixed with 100% cold methanol. Non-crosslinked lipids and cleaved coumarin were extracted with methanol:chloroform:acetic acid (55:10:0.75). Lipid location was determined after click chemistry of Alexa 568—picolyl azide (green). A) Without exposure to 350 nm light, most of the lipid was washed away during fixation. B) Increased uncaging time led to more lipid detectable at the plasma membrane (arrows). The images are representative of two independent sets of experiments. Scale bar = 20 μm.

All proteomic data were acquired in triplicate with or without exposure to UV light or without addition of a lipid derivative. Cells were fractionated into membrane and cytosolic fractions. Each fraction was investigated independently. Hits were selected if a protein showed an increase in spectral counts larger than 1.2-fold (log2 of 0.36) between UV and −UV conditions (−UV means no uncaging and cross-linking) or between + UV and control (no compound added but cells exposed to UV light). We chose spectral counts as a readout to permit the comparison to other proteomic analyses from our lab using multifunctional lipids.[10b,12] Hit proteins were only found in the membrane fraction. They had to appear in at least two of the three experimental repeats and had to feature a lipid-binding domain (Figure 6). Following these very strict criteria, we identified six proteins. Three of them (MPP6, SDCBP and ATP11A (Table 1, Table S1)) were known to be involved in lipid transport[20] or are involved in protein trafficking or membrane organization,[21] respectively. They were selected as putative PI(3,4,5)P_3 derivate transporters and were investigated by RNAi knock down experiments. By testing the hypothesis that active transport is involved in trafficking of 3-phosphorylated phosphoinositides from endomembranes to the plasma membrane, we found that an RNAi against MPP6 and ATP11A but not SDCBP significantly delayed appearance of multifunctional PI(3,4,5)P_3 at the plasma membrane (Figure 7, Figure S5).

Although the presented experiments are incomplete with respect to all hits from the proteomic screen, the results strongly support active transport of PI(3,4,5)P_3 from endomembranes to the plasma membrane. This phenomenon might explain how cells are able to maintain a steep PI(3,4,5)P_3 gradient over its quite closely connected membrane systems. The results also support the observation that PH domains predominantly recognize PI(3,4,5)P_3 at the plasma membrane.[22] A broader study investigating other protein hits of the screen as well as the transport of other 3-phosphorylated phosphoinositides will be performed in the future.

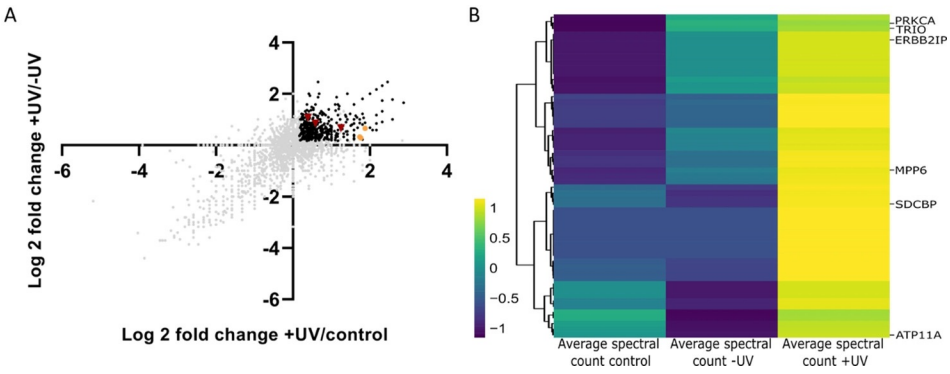

Figure 6. Visualization of protein hits. A) Scatter blot of all proteins with increased spectral counts in UV over -UV conditions vs. UV over control (no lipid, but UV exposure) conditions (black dots). Those with a lipid-binding domain are colored; the ones in orange were investigated as putative transport proteins by RNAi. B) Heat map of the 60 proteins that we identified as hits with most confidence (for more details, see Suppl. Figures S3 and S4). Values in the heat map are scaled by row for easier visualization.

Table 1: Putative lipid transport proteins detected by proteomic analysis after photo-crosslinking of TF-PI(3,4,5)P_3 and subsequent attachment to azide beads via click chemistry. Ratio increase and standard error were determined from three independent repeats.

	Average spectral count control	Average spectral count −UV	Average spectral count +UV	Fold change +UV/control	Fold change +UV/−UV
MAGUK p55 subfamily member 6 (MPP6)	4.333333	2.333333	6	1.384615	2.571429
Probable phospholipid-transporting ATPase IH (ATP11A)	3	5	8.5	2.833333	1.7
Syntenin-1 (SDCBP)	3	2.333333	5	1.666667	2.142857

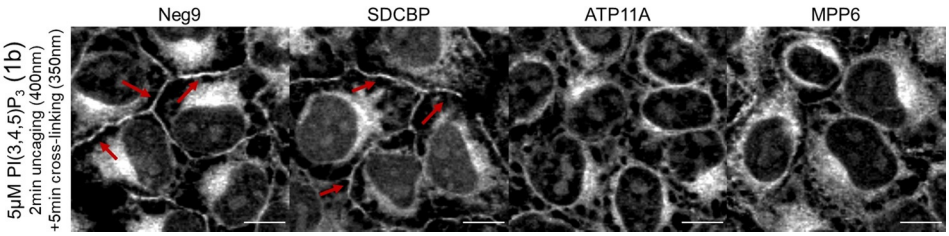

Figure 7. Location of uncaged, photo-crosslinked and fluorescently tagged PI(3,4,5)P_3 in fixed cells previously transfected with an RNAi against putative lipid transport proteins listed in Table 1. Neg9 = random siRNA control. The knock-down of ATP11A and MPP6, respectively, but not SDCBP, led to persisting residence times of PI(3,4,5)P_3 in endomembranes. This suggests that these proteins are actively involved in phosphoinositide transport to the plasma membrane. The images are representative of three independent experiments. Red arrows points to plasma membrane staining through the fluorescently tagged lipid. Scale bar = 10 μm.

Conclusion

In conclusion, we prepared multifunctional derivatives of PI(3,4)P_2 and PI(3,4,5)P_3. The functional modifications did not prevent biological activity with respect to receptor internalization, although this needs to be demonstrated again for a wider set of conditions. The multifunctional lipid derivatives will be exceptional discovery tools as for the first time their use will provide a comprehensive overview of 3-*O*-phosphorylated phosphoinositide binding proteins under various conditions. The current observation that the phosphoinositide derivatives are binding to putative lipid transport proteins opens new views on how phosphoinositides distribute in cells. Phosphoinositide transport by proteins is well established for phosphatidylinositol 4-phosphate.[23] However, trafficking of 3-*O*-phosphorylated phosphoinositides represents a novel aspect in lipid signaling. The results demonstrate the discovery tool character of the multifunctional lipid derivatives.

Acknowledgements

We gratefully acknowledge funding from the NIH (R01GM127631) and Transregio 186, funded by the German Research Foundation (DFG). We thank the EMBL proteomics facility for the analysis of the proteomics data, especially Dr Per Haberkant and Dr Frank Stein. We also thank Dr Sergio Triana for his help with the creation of the heat map plots. Open access funding enabled and organized by Projekt DEAL.

Conflict of Interest

The authors declare no conflict of interest.

Keywords: caged compounds · cell imaging · lipid transport · phosphoinositides · photo-crosslinking

[1] a) T. Balla, *Physiol. Rev.* **2013**, *93*, 1019 – 1137; b) R. R. Madsen, B. Vanhaesebroeck, *Sci. Signaling* **2020**, *13*, eaay2940.

[2] M. R. Hokin, L. E. Hokin, *J. Biol. Chem.* **1953**, *203*, 967 – 977.

[3] a) A. E. Traynor-Kaplan, A. L. Harris, B. L. Thompson, P. Taylor, L. A. Sklar, *Nature* **1988**, *334*, 353 – 356; b) M. Whitman, C. P. Downes, M. Keeler, T. Keller, L. Cantley, *Nature* **1988**, *332*, 644 – 646.

[4] H. Wang, D. Loerke, C. Bruns, R. Muller, P. A. Koch, D. Puchkov, C. Schultz, V. Haucke, *J. Biol. Chem.* **2020**, *295*, 1091 – 1104.

[5] V. Laketa, S. Zarbakhsh, A. Traynor-Kaplan, A. Macnamara, D. Subramanian, M. Putyrski, R. Mueller, A. Nadler, M. Mentel, J. Saez-Rodriguez, R. Pepperkok, C. Schultz, *Sci. Signaling* **2014**, *7*, ra5.

[6] Y. Posor, M. Eichhorn-Gruenig, D. Puchkov, J. Schöneberg, A. Ullrich, A. Lampe, R. Müller, S. Zarbakhsh, F. Gulluni, E. Hirsch, M. Krauss, C. Schultz, J. Schmoranzer, F. Noé, V. Haucke, *Nature* **2013**, *499*, 233 – 237.

[7] P. Várnai, G. Gulyás, D. J. Tóth, M. Sohn, N. Sengupta, T. Balla, *Cell Calcium* **2017**, *64*, 72 – 82.

[8] a) M. A. Lemmon, *Nat. Rev. Mol. Cell Biol.* **2008**, *9*, 99 – 111; b) J. G. Pemberton, T. Balla, *Adv. Exp. Med. Biol.* **2019**, *1111*, 77 – 137.

[9] C. Wang, J. P. Palavicini, M. Wang, L. Chen, K. Yang, P. A. Crawford, X. Han, *Anal. Chem.* **2016**, *88*, 12137 – 12144.

[10] a) P. Haberkant, F. Stein, D. Höglinger, M. J. Gerl, B. Brügger, P. P. Van Veldhoven, J. Krijgsveld, A. C. Gavin, C. Schultz, *ACS Chem. Biol.* **2016**, *11*, 222 – 230; b) D. Höglinger, A. Nadler, P. Haberkant, J. Kirkpatrick, M. Schifferer, F. Stein, S. Hauke, F. D. Porter, C. Schultz, *Proc. Natl. Acad. Sci. USA* **2017**, *114*, 1566 – 1571; c) A. Nadler, G. Reither, S. Feng, F. Stein, S. Reither, R. Muller, C. Schultz, *Angew. Chem. Int. Ed.* **2013**, *52*, 6330 – 6334; *Angew. Chem.* **2013**, *125*, 6455 – 6459; d) M. Schuhmacher, A. T. Grasskamp, P. Barahtjan, N. Wagner, B. Lombardot, J. S. Schuhmacher, P. Sala, A. Lohmann, I. Henry, A. Shevchenko, U. Coskun, A. M. Walter, A. Nadler, *Proc. Natl. Acad. Sci. USA* **2020**, *117*, 7729 – 7738; e) M. J. Niphakis, K. M. Lum, A. B. Cognetta 3rd, B. E. Correia, T. A. Ichu, J. Olucha, S. J. Brown, S. Kundu, F. Piscitelli, H. Rosen, B. F. Cravatt, *Cell* **2015**, *161*, 1668 – 1680.

[11] R. Müller, M. Citir, S. Hauke, C. Schultz, *Chem. Eur. J.* **2020**, *26*, 384 – 389.

[12] P. Haberkant, R. Raijmakers, M. Wildwater, T. Sachsenheimer, B. Brügger, K. Maeda, M. Houweling, A. C. Gavin, C. Schultz, G. van Meer, A. J. Heck, J. C. Holthuis, *Angew. Chem. Int. Ed.* **2013**, *52*, 4033 – 4038; *Angew. Chem.* **2013**, *125*, 4125 – 4130.

[13] a) D. Höglinger, A. Nadler, C. Schultz, *Biochim. Biophys. Acta Mol. Cell Biol. Lipids* **2014**, *1841*, 1085 – 1096; b) A. Laguerre, C. Schultz, *Curr. Opin. Cell Biol.* **2018**, *53*, 97 – 104.

[14] a) F. Hövelmann, K. M. Kedziora, A. Nadler, R. Müller, K. Jalink, C. Schultz, *Cell Chem. Biol.* **2016**, *23*, 629 – 634; b) A. Laguerre, S. Hauke, J. Qiu, M. J. Kelly, C. Schultz, *J. Am. Chem. Soc.* **2019**, *141*, 16544 – 16547.

[15] a) M. Mentel, V. Laketa, D. Subramanian, H. Gillandt, C. Schultz, *Angew. Chem. Int. Ed.* **2011**, *50*, 3811 – 3814; *Angew. Chem.* **2011**, *123*, 3895 – 3898; b) D. Subramanian, V. Laketa, R. Müller, C. Tischer, S. Zarbakhsh, R. Pepperkok, C. Schultz, *Nat. Chem. Biol.* **2010**, *6*, 324 – 326.

[16] C. Schultz, *Bioorg. Med. Chem.* **2003**, *11*, 885 – 898.

[17] C. Dinkel, M. Moody, A. Traynor-Kaplan, C. Schultz, *Angew. Chem. Int. Ed.* **2001**, *40*, 3004 – 3008; *Angew. Chem.* **2001**, *113*, 3093 – 3096.

[18] A. B. Neef, C. Schultz, *Angew. Chem. Int. Ed.* **2009**, *48*, 1498 – 1500; *Angew. Chem.* **2009**, *121*, 1526 – 1529.

[19] A. Grabon, V. A. Bankaitis, M. I. McDermott, *J. Lipid Res.* **2019**, *60*, 242 – 268.

[20] K. Segawa, S. Kurata, S. Nagata, *J. Biol. Chem.* **2016**, *291*, 762 – 772.

[21] a) J. M. Beekman, P. J. Coffer, *J. Cell Sci.* **2008**, *121*, 1349 – 1355; b) F. Ye, M. Zeng, M. Zhang, *Curr. Opin. Struct. Biol.* **2018**, *48*, 6 – 15.

[22] W. S. Park, W. D. Heo, J. H. Whalen, N. A. O'Rourke, H. M. Bryan, T. Meyer, M. N. Teruel, *Mol. Cell* **2008**, *30*, 381 – 392.

[23] J. Chung, F. Torta, K. Masai, L. Lucast, H. Czapla, L. B. Tanner, P. Narayanaswamy, M. R. Wenk, F. Nakatsu, P. De Camilli, *Science* **2015**, *349*, 428 – 432.

Manuscript received: March 12, 2021
Revised manuscript received: May 7, 2021
Accepted manuscript online: June 1, 2021
Version of record online: July 26, 2021

